



Adsorption of the First-Line Covid Treatment Analgesic onto Activated Carbon from Residual Pods of *Erythrina Speciosa*

Jordana Georjin¹ · Dison S. P. Franco² · Matias S. Netto³ · Mohammad Saood Manzar⁴ · Mukarram Zubair⁴ · Lucas Meili⁵ · Daniel G. A. Picilli¹ · Luis F. O. Silva²

Received: 9 May 2022 / Accepted: 30 August 2022 / Published online: 10 September 2022
© The Author(s), under exclusive licence to Springer Science+Business Media, LLC, part of Springer Nature 2022

Abstract

In this study, the residual pods of the forest species *Erythrina speciosa* were carbonized with $ZnCl_2$ to obtain porous activated carbon and investigated for the adsorptive removal of the drug paracetamol (PCM) from water. The PCM adsorption onto activated carbon is favored at acidic solution pH. The isothermal studies confirmed that increasing the temperature from 298 to 328 K decreased the adsorption capacity from 65 mg g^{-1} to 50.4 mg g^{-1} ($C_0 = 175 \text{ mg L}^{-1}$). The Freundlich model showed a better fit of the equilibrium isotherms. Thermodynamic studies confirmed the exothermic nature ($\Delta H^0 = -39.1066 \text{ kJ mol}^{-1}$). Kinetic data indicates that the external mass transfer occurs in the first minutes followed by the surface diffusion, considering that the linear driving force model described the experimental data. The application of the material in the treatment of a simulated effluent with natural conditions was promising, presenting a removal of 76.45%. Therefore, it can be concluded that the application of residual pods of the forest species *Erythrina speciosa* carbonized with $ZnCl_2$ is highly efficient in the removal of the drug paracetamol and also in mixtures containing other pharmaceutical substances.

Keywords Residual pod · Drug removal · Adsorption of pollutants · Emergent pollutants

Introduction

The presence of different pharmaceutical compounds in the environment has been the subject of several studies since

they are generally polar and water-soluble molecules (Madden et al. 2009). Paracetamol is widely employed worldwide for relieving pain and reducing fever or temperature in the body (Sundararaman et al. 2022). The detection of these types of drugs normally occurs at low concentrations (fluctuating from $\mu\text{g L}^{-1}$ to ng L^{-1}) (Hollender et al. 2008), however, long-term exposure by living organisms can cause aquatic toxicity, development of resistance in pathogenic microbes, genotoxicity, and endocrine disruption (Khetan and Collins 2007; Fessard and Le Hégarat 2010). Hence a lot of studies have primarily focused on the detection of pharmaceutical contamination in various kinds of water sources like surface water, underground water, and drinking water (Sundararaman et al. 2022; Jari et al. 2022).

The main drugs found in wastewater normally do not require controlled prescriptions, and this class includes analgesics, muscle relaxants, and hormonal drugs (Xu et al. 2009). Acetaminophen or paracetamol is one of the most consumed analgesics worldwide, as it is cheap and effective, with low side effects and few contraindications (Bertolini et al. 2006; Žur et al. 2018). In late 2019, an epidemic of the human coronavirus disease 2019 (COVID-19) was

Supplementary information The online version contains supplementary material available at <https://doi.org/10.1007/s00267-022-01716-6>.

✉ Lucas Meili
lucas.meili@ctec.ufal.br

- ¹ Department of Civil and Environmental Engineering, Federal University of Santa Maria, UFSM, Santa Maria, Brasil
- ² Department of Civil and Environmental Engineering, Universidad de la Costa, CUC, Calle 58 # 55–66, Barranquilla, Atlántico, Colombia
- ³ Department Chemical Engineering, Federal University of Santa Maria, 97105–900 Santa Maria, Brazil
- ⁴ Department of Environmental Engineering, College of Engineering, Imam Abdulrahman Bin Faisal University, P.O. Box 1982, Dammam 31451, Saudi Arabia
- ⁵ Laboratory of Process, Center of Technology, Federal University of Alagoas, Maceió, AL, Brazil

reported in Wuhan, China, one of the world's most densely populated cities with a population of over eleven million people (Nandan et al. 2021). Since then, COVID-19 has become a major global public health issue that has had a significant impact on global social development and continues to pose a significant challenge to global public health systems (Guo et al. 2022). In 2020, paracetamol consumption was even higher and is recommended as the first-line treatment for fevers caused by the common cold, flu, and coronavirus (COVID-19) (Sohrabi et al. 2020; Goscianska et al. 2021). The main form of PCM disposal in water bodies is through urine since approximately 65% of the drug consumed is not absorbed by the human body (Lima et al. 2019; Żur et al. 2018). These factors caused PCM concentrations to be detected in the ranges of 20–4300 ng L⁻¹ and 78170 ng L⁻¹, these values exceed concentrations considered not dangerous to living organisms (above 9200 ng L⁻¹) (Bertolini et al. 2006; Dai et al. 2019). Studies report that when PCM persists in the environment can degrade releasing toxic, carcinogenic, and mutagenic compounds, due to this, studies that bring solutions that remove PCM before its discharge into the environment are of high relevance (Pi et al. 2017).

The key techniques that are used to remove pharmaceuticals from the water phase includes degradation (Addamo et al. 2005), coagulation-flocculation (Wang et al. 2022), membrane (Katibi et al. 2021), oxidation (Siedlecka et al. 2018), filtration (Siedlecka et al. 2018) and adsorption (Saood Manzar et al. 2022; Khan et al. 2022). The adsorption technique is done with the use of activated carbon from the plant residues and has been successfully used to remove several pharmaceutical compounds (Chakraborty 2014; Georgin et al. 2021). The great advantage of these studies are that they incorporate a very little cost for obtaining residual biomass, employ a simple method of operation and also have a low cost of implementation (Wong et al. 2018). Furthermore, when a regeneration strategy is used for the reutilization of the spent adsorbent, adsorption does not create harmful compounds as a result of its operation (Quintela et al. 2020; Bernal et al. 2021). Various kinds of carbon-based materials like biochar-based adsorbents (Zubair et al. 2020, 2022), activated carbon (Alagha et al. 2020), hydrochar (Mestre et al. 2015), green coffee residues (Manzar et al. 2020), tree leaves (Liakos et al. 2021; de et al. 2022), coconut shells (Bello et al. 2020) and date palm ash (Blaisi et al. 2018) have been effectively employed to eliminate pollutants from the water phase. For instance, Tunç et al (Tunç et al. 2021) used sawdust-based activated carbon for the removal of paracetamol from the aqueous phase. The author established the developed adsorbent could effectively remove 99.24% of the drug within 90.52 min. In another study activated moringa seed pod was used to effectively remove paracetamol from the

water phase (Ogunmodede et al. 2021). Similarly in another investigation, an author studied about the removal of paracetamol using expended coffee grounds (Benyekkou et al. 2020). The fabricated material owing to its high specific surface area (888.1 m²/g), presence of functional groups on the adsorbent surfaces was anticipated to enable strong interface with pollutant molecules. Therefore, using carbon based adsorbent as cheap sustainable adsorbent may assist from an cost-effective and other perspective.

Erythrina used in this study is a genus of the botanical family Leguminosae (*Fabaceae*), which occurs throughout the Brazilian territory. They are medium-sized trees, soft-wood, large red or orange flowers, which occur in a wide variety of habitats, from tropical forests to high altitude forests (Fahmy et al. 2018). Its fruits and seeds are dispersed by the action of the wind. They are distributed in the Americas and Africa. In Brazil, about 12 species of *Erythrina* are found, with the species *Erythrina speciosa* being the most used for medicinal purposes (Medina et al. 2009; Konozy et al. 2003). This species can reach 20 m in height, presenting compound leaves, long petiolate (de et al. 2019). It loses all its leaves at the time of flowering, covering itself with orange inflorescences. Its growth is fast and is normally used in the urbanization of squares and parks. It produces pod-like fruits, which vary from 15 to 30 cm and are light brown. Its fruits are not edible and because they do not have a pleasant aroma and color, they are also not attractive to birds, therefore, when ripe, they dry and fall, generating a large amount of organic biomass over the soil (da et al. 2014). No studies in the literature have been found related to the use of pods for the removal of emerging pollutants from an aqueous medium.

In this work, the adsorptions of paracetamol were estimated via activated carbon prepared from residual pods of the species *Erythrina speciosa* carbonized with zinc chloride (ZnCl₂) as an activator. The *Erythrina speciosa* pod residues and the carbonized material were characterized by their functional groups, morphology, and atom mass percentage. pH and adsorbent dosage studies were also determined. Finally, isothermal and kinetic studies were conducted to investigate the PCM adsorption and the activated carbon was also employed in the treatment of simulated effluent.

Material and Methods

Chemicals and Reagents

For the development of activated carbon and the adsorption tests, several reagents were used, all obtained by the company Sigma-Aldrich-USA, and presenting analytical grades. The chemical compounds used were: ZnCl₂ (zinc chloride),

HCl (hydrochloric acid), and $C_8H_9NO_2$ (paracetamol; molecular weight: $151.163 \text{ g mol}^{-1}$, $\lambda_{\text{max}} = 257 \text{ nm}$). For the preparation of different concentrations of PCM, a stock solution was prepared by diluting 2 g L^{-1} of the drug in methanol (10%). The following solutions were obtained by diluting the stock solution and stored in glass vials. All samples were prepared with deionized water. The initial pH adjustment of each solution was carried out with NaOH and HCl at 0.10 mol L^{-1} and using a pH meter.

Pyrolysis of *Erythrina sp.* and Characterization

Pods of the *Erythrina sp.* species were directly collected - from the soil, in the city of Santa Maria in the state of Rio Grande do Sul-Brazil. About 1 kg of collected material was taken directly to the laboratory, where each pod was washed with tap water, ensuring that all impurities were removed, then the material was manually broken into 5 cm pieces, and transferred to the dry oven for 24 h set at a temperature of 323.15 K. After that, the pods were grounded using a knife mill. The obtained material showed a brown color and was sieved using an opening of $250 \mu\text{m}$, and labeled as grounded *Erythrina sp.* pod residues. Last, 5 g of the material was separated for characterization and the remains were - employed in the fabrication of the activated carbon.

In the carbonization process, about 50 g of the ground *Erythrina sp.* pod residues were mixed with 50 g of zinc chloride ($ZnCl_2$), and 2 mL of deionized water. After that, the samples were dried for 12 h. The dried powder sample was transferred to a quartz reactor. The reactor was coupled in the oven under N_2 atmosphere at a flow rate of 0.25 L min^{-1} . A heating ramp of $283.15 \text{ K min}^{-1}$, the maximum temperature of 1073.15 K, and the pyrolysis time of 120 min was employed. Sequentially, the activated carbon was washed with HCl solution (10 mol L^{-1}) and finally with distilled water to ensure the removal of unreacted $ZnCl_2$ on the surface of activated carbon. This step was conducted several times until neutral pH of water is obtained. The material was finally separated through decantation and followed by drying for 3 h at 323.15 K. The yield of the activated carbon and the characterization of the materials are shown in Supplementary Materials S1 and S2, respectively.

PCM Adsorption Experiments

The PCM batch adsorption experiments on the developed activated carbon were conducted in a thermostatic stirrer (Marconi, MA093, Marconi, Brazil) at 160 rpm. The determination of the residual PCM concentration after batch experiment was done by employing a spectrophotometer (UV mini 1240, Shimadzu, Japan) set at wavelength of 257 nm. The residual PCM solution was first centrifuged

(CentriBio, 80-2B, Brazil) for 25 min at 4000 rpm, to separate the spent activated carbon before measurement in spectrophotometer.

First, the optimum pH of the solution was determined. For this purpose, four Erlenmeyer flasks were used, adjusted to pH ranges of 3, 5, 7, and 9, in 50 mL of PCM solution at a concentration of 45 mg L^{-1} . The samples were shaken for 2 h with the dosage of 1 g L^{-1} of activated carbon. After the determination of the pH, the optimum adsorbent dosage was determined by taking about 0.4, 0.6, 0.8, 1, and 1.2 g L^{-1} of adsorbent, containing 50 mL of 45 mg L^{-1} of PCM solution. Before stirring, the solutions were adjusted to the ideal pH. Further adsorption experiments (isotherms and kinetics) were performed at optimal adsorption conditions (pH = 3, 0.8 g L^{-1}).

For the adsorption equilibrium curves, the adsorption experiments were carried out under the following conditions; temperatures (298, 308, 318, and 328) K, initial concentrations of PCM (25, 50, 100, 150, and 175 mg L^{-1} , contact time 5 h in 50 mL Erlenmeyer flasks. Finally, the kinetic studies were carried out at varying initial concentrations of PCM from 25, 50 and 100 mg L^{-1} in 50 mL Erlenmeyer flasks of solution at a room temperature of approximately 298 K. The samples were collected with the aid of an aliquot of 5 ml at time intervals of 0, 10, 20, 30, 60, 120 and 180 min. The standard adsorption equations (Supplementary Material S3) were employed for the adsorption capacity at any time (q_t , mg g^{-1}), adsorption at equilibrium (q_e , mg g^{-1}), and the percentage of removal (R, %) determination.

Equilibrium and Thermodynamic Calculations

The adsorption isotherms are essential to evaluate the adsorption behavior of pollutant molecules on the surface of adsorbent. In this work the following models were chosen: Freundlich (Freundlich 1907), Dubinin-Radushkevich (Dubinin et al. 1971), Temkin (Temkin and Pyzhev 1939), Langmuir (Langmuir 1918). Similarly, the thermodynamic parameters were estimated according to the methodology proposed by Tran et al (Tran et al. 2017). The chosen models are depicted in the Supplementary Materials (S3 and S4).

Modeling Adsorption Kinetics

In this work, the linear driving force (LDF) model (Glueckauf 1955) was chosen to represent adsorption data. The LDF takes into consideration that the adsorption kinetics/ concentration decay curve is dependent on the adsorption in equilibrium and the surface diffusion of the system. The LDF model is presented in Eqs. 1–3. The model description and derivation are depicted in

Supplementary Material S5.

$$\frac{dC_t}{dt} = k_{LDF} \left(C_0 - C_t - D_0 \left(K_F C_e^{1/n} \right) \right) \quad (1a)$$

$$C_t(t = 0) = C_0 \quad (1b)$$

$$\frac{dq_t}{dt} = - \frac{1}{D_0} \frac{dC_t}{dt} \quad (2)$$

$$D_s = \frac{R_p^2 k_{LDF}}{15} \quad (3)$$

where k_{LDF} is the mass transfer coefficient according to the initial concentration (min^{-1}), t is time (min), D_0 is the adsorbent dosage (g L^{-1}), C_t is the PCM concentration at any time (mg L^{-1}), C_0 is the PCM initial concentration (mg L^{-1}), $1/n$ is the Freundlich exponent (dimensionless), K_F is the Freundlich constant ($(\text{mg g}^{-1}) (\text{mg L}^{-1})^{-1/n}$), C_e is the PCM concentration at the equilibrium (mg L^{-1}), q_t is PCM adsorption capacity at determined time (mg g^{-1}), D_s is the surface diffusion ($\text{cm}^2 \text{s}^{-1}$), R_p is the adsorbent

LDF Solution, Parameters Estimation, and Model Evaluation

The solution of LDF was performed using Matlab, for this the built-in function *ode15s* was employed coupled with *nlinfit* (nonlinear fit) for the estimation of the parameters, initial guess value was done through trial and error. For the isotherms first, the *particleswarm* function was employed for the initial guessing value, e.g for the adsorption capacity (q_{par}): $0 \geq q_{\text{par}} \leq q_{\text{exp}}$, and for the isotherm constants (k_{par}): $0 \leq k_{\text{par}} \leq 1$. After the initial guess, the values were employed in the *nlinfit* or the *lsqnonlin* (nonlinear fit with bounds) as the initial guess for the determination of the isotherm model parameters. Regarding the evaluation of the models, it was done by employing statistical indicators as shown in Supplementary Material S6.

Synthetic Effluent Simulation Based on Pharmaceutical Mixture and Salts

To further evaluate the possible application of the activated carbon in the treatment of a mixture of pharmaceuticals and salts, the adsorbent was employed in the treatment of a simulated effluent. The composition of the simulated effluent (100 mL) is shown in Table S1. For the experiment, a dosage of 2 g L^{-1} was employed, considering that the optimal dosage found for the single experiment was not enough to achieve a high percentage of removal. Other experimental conditions were: agitation for 4 h at 180 rpm (298 K). For the determination of the spectrum curves before and after the adsorption, a spectrophotometer was

employed (SP-22, Biospectro, Brazil). The area under the curve before and after the adsorption was used for the estimation of the percentage of removal using the Origin 2016 software.

Results and Discussion

Characterization of Erythrina sp. pod Residues and Activated Carbon

The activated carbon prepared from the pyrolysis of ZnCl_2 mixed residual pods of the forest species *Erythrina sp.* obtained a yield close to 29%. Taking into account that the residual biomass has around 70% of volatile material, which was eliminated during pyrolysis with ZnCl_2 . The ash content was close to 5%, indicating the produced activated carbon was mainly composed of ash and carbon, results that are in agreement with X-ray spectroscopy (Fig. 2b). This yield is in agreement with other studies that employed biomass residues as precursor materials and zinc chloride as an activating agent (Georgin et al. 2021; Franco et al. 2021; Kerkhoff et al. 2021).

Interestingly, activated carbon presented a satisfactory surface area of $795.109 \text{ m}^2 \text{ g}^{-1}$, where the N_2 adsorption/desorption isotherms and pore size distribution are shown in Fig. 1A. Considering the IUPAC classification, nitrogen isotherms are type I, with hysteresis loops between $p/p_0 = 0.1-0.8$, according to the classification these isotherms correspond to micro and mesoporous structures (Zhang et al. 2016). At low relative pressures, the adsorption of N_2 isotherms increases rapidly, while at moderate pressures the adsorption decreases, indicating that the carbon structure is micro and mesoporous (Zhang et al. 2016). Figure 1B indicates that the average pore diameter was 1.2320 nm for a total pore volume of $0.422 \text{ cm}^3 \text{ g}^{-1}$. Taking into consideration that the PCM size is 9.416 \AA the pore size of the activated carbon is large enough to allow the internal mass transfer and adsorb the PCM.

The FTIR of the *Erythrina sp. pod residues* and activated carbon was performed to identify the functional groups present on the surface (Fig. 2a). First, the broadband at (a) correspond to OH groups, -present in both samples, however with less intensity in the activated carbon (Puchana-Rosero et al. 2016). The region in (b) present in both materials corresponds to the conjugate elongation of $\text{C}=\text{O}$ of the lignin structure (Fontana et al. 2016). The region in (c) appeared only in the residues corresponds to the $\text{C}-\text{O}$ stretch of acetyl groups present in lignin (Rahman et al. 2019). Finally, the band in region (d), observed in both spectra, but with lower intensity in the pyrolyzed sample associated to stretching vibrations such as CN or CO (Pereira et al. 2003). The study by Salomon et al., (de et al.

Fig. 1 N₂ adsorption-desorption isotherms (A) and pore size distribution (B) for the developed activated carbon

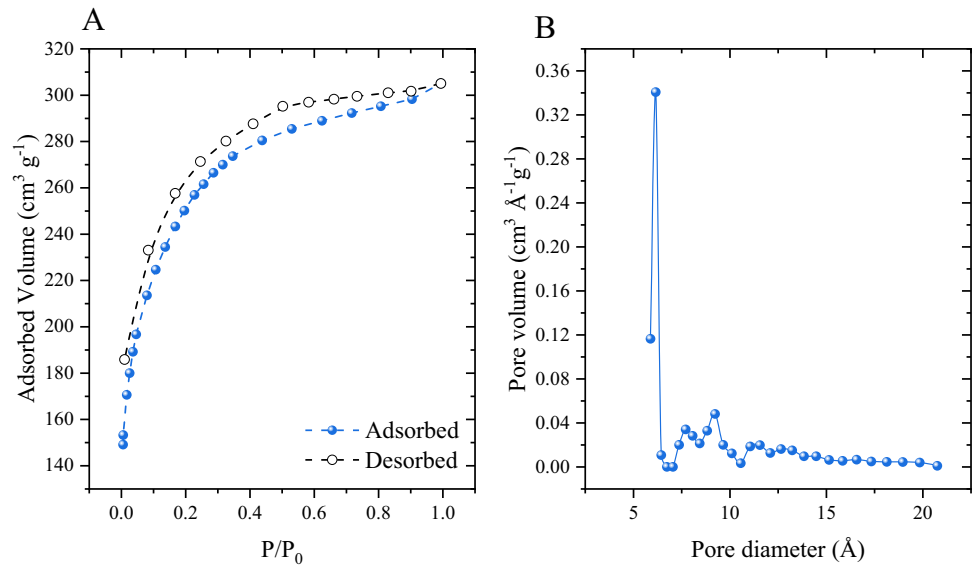
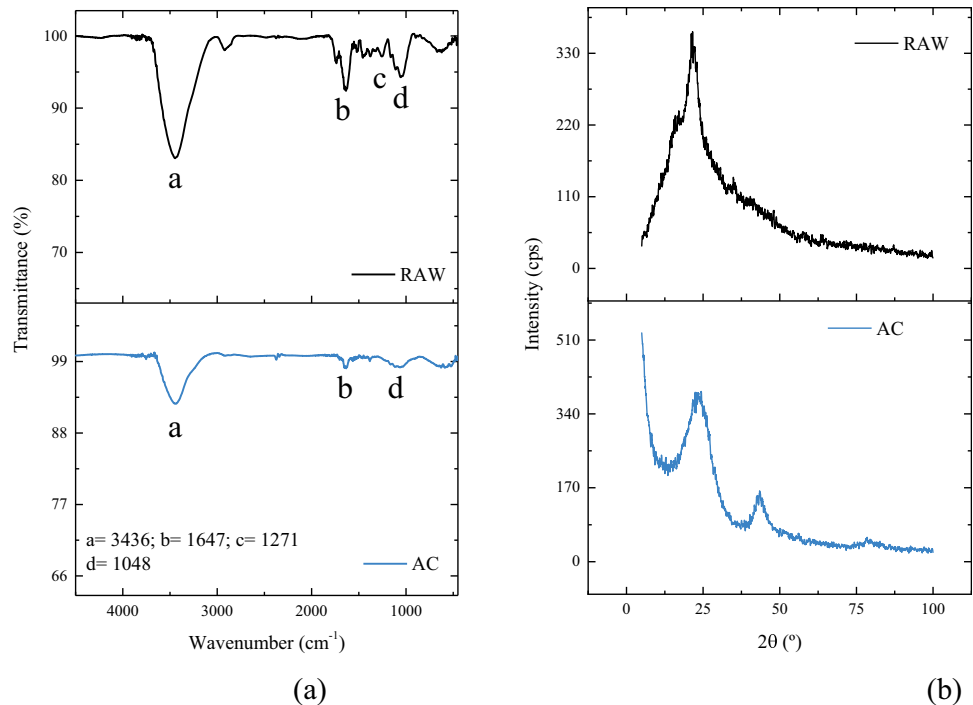


Fig. 2 a FTIR spectra and (b) XRD for Erythrina sp. pod residues (RAW) and the activated carbon



2021) also observed the elimination of several bands on the surface of the material pyrolyzed with ZnCl₂. Most of the groups present are composed of hydroxyl and carbonyl, which are fundamental molecules that constitute lignin and cellulose (Adebisi et al. 2017). Another point to be highlighted is that the presence of aromatic rings corresponding to C=C bonds was not observed in the carbonaceous material. It is worth mentioning that these bonds help in the π - π interactions during the adsorption process. Therefore, probably the interactions that occurred between the

adsorbent and the PCM molecules are hydrogen bonds or electrostatic interactions (Spessato et al. 2019).

Figure 2b corresponds to the diffraction patterns of both materials. The XRD results showed that the materials exhibited broad and amorphous peaks related to amorphous carbon at 22.1° for the precursor material and around 21.5° for the activated carbon. Additionally, a smaller peak at 45°, corresponding to the graphitic carbon structure was also observed in activated carbon (Oksman et al. 2006). Predominantly amorphous structures are disorganized and do

not present an ordered structural arrangement, where these spaces with disordered sizes and shapes can favor the accommodation of the adsorbate molecules.

To obtain more information regarding the chemical elements present in the materials, EDS analyzes were performed (Fig. S1). The percentages of the elements Ca, Mg, and K present in the original material were below 1%, indicating that in their original form the residual pods are formed by carbon (61.89%) and oxygen (28.69%), as shown in Fig. S1a. The carbonization process involves a substantial loss of volatile matter, where the percentage of carbon was increased to 88.85%, and oxygen decreased to 9.87% (Fig S1b). Another point to be analyzed is that although some studies in the literature confirm a small amount of Zn (Cruz et al. 2018; Danish et al. 2018), in this study all zinc was completely removed from the activated carbon after activation.

The SEM for the *Erythrina sp.* pod residues and activated carbon samples are depicted in Fig. S2. Figures A and B represent the original material and figures C and D are for activated carbon. It is evident that the particles remained with varying sizes and irregular shapes (2A and 2C), however, the surface of the activated carbon exhibited more irregularities and voids compared to the original material (2B and 2D) which provide active sorption sites for removal of pharmaceuticals from water. Previous studies confirmed that pyrolysis followed by chemical activation with ZnCl_2 causes morphological changes in materials of plant origin, such as eucalyptus residues (Han et al. 2020), olive pits (Baldoni et al. 2020), leaves of folium cycas (Kong et al. 2020), peanut husks (Georgin et al. 2016), seed pods of *Jacaranda mimosifolia* (Georgin et al. 2021), fruit residues from the *Ceiba sp.* forest species (Franco et al. 2021), *Diospyros kaki* fruit residues (Salomón et al. 2022), residues from the mushroom *Agaricus bisporus* (Lazarotto et al. 2021) and residual peel of pitaya fruit (Georgin et al. 2022).

Effect of pH and Adsorbent Dosage

The initial solution pH is regarded as highly important parameter in the adsorption process since it can influence the electrical charges on the surface of the adsorbent, as well as cause the ionization of the molecules present in the adsorbate (Spessato et al. 2019). Figure 3a shows the effect of solution pH ranging from 3 to 9 on PCM adsorption on the surface of activated carbon and the speciation of the PCM. It is evident that the solution pH showed a great influence on the adsorption of the PCM, obtaining high adsorption capacity values at the lowest solution pH ($Q_{\text{max}} = 37.12 \text{ mg g}^{-1}$), and linearly decreased as the pH was increased, with the lowest capacity ($Q_{\text{max}} = 16.58 \text{ mg g}^{-1}$) obtained at pH 9, thus from these results, a solution pH value of 3 was selected for the following adsorption studies.

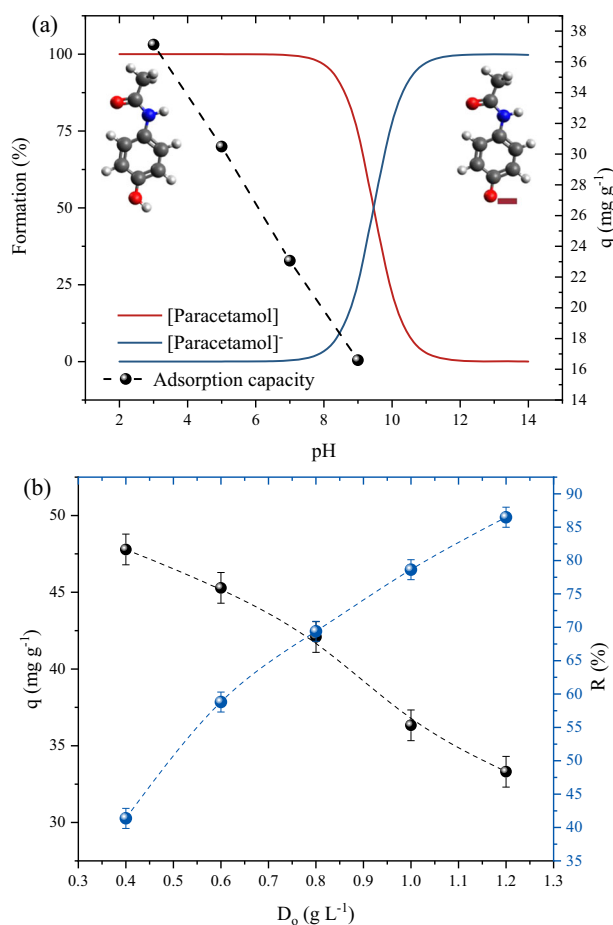


Fig. 3 **a** pH solution effect on PCM adsorption and speciation curves for the PCM ($V = 50 \text{ mL}$, $T = 298 \text{ K}$, $D_{\text{ads}} = 1 \text{ g L}^{-1}$, $C_0 = 45 \text{ mg L}^{-1}$, $t = 120 \text{ min}$); and **b** effect of adsorbent dosage on PCM adsorption ($V = 50 \text{ mL}$, $T = 298 \text{ K}$, $\text{pH} = 3$, $C_0 = 45 \text{ mg L}^{-1}$, $t = 120 \text{ min}$)

From the speciation diagram, it is expected that the PCM molecules are found in neutral form, from pH 2 to 7, and PCM molecules start to ionize due to the pH effects above $\text{pH} > 7$. The type of PCM molecule directly affects what type of physical or chemical interactions governed the PCM and the activated carbon interface. The adsorption mechanism is further discussed in section 3.5.

In addition, to the pH effect, the adsorbent dosage is also important to the adsorption study, leading to information regarding its viability. In other words, the material consumption about the adsorption capacity and percentage of removal. The effect of adsorbent dosage on PCM adsorption was evaluated at different activated carbon dosages (0.4, 0.6, 0.8, 1, and 1.2 g L^{-1}), at a solution pH of 3, contact time of 120 min and temperature 298 K. Figure 3b depicts the results of the dosage effect, regarding adsorption capacity and the percentage removal of PCM. It was observed that as the adsorbent dosage increased from 0.4 to 1.2 g , the percentage of removal increased from 41.36 to 86.49%. This effect is explained by the availability of the active

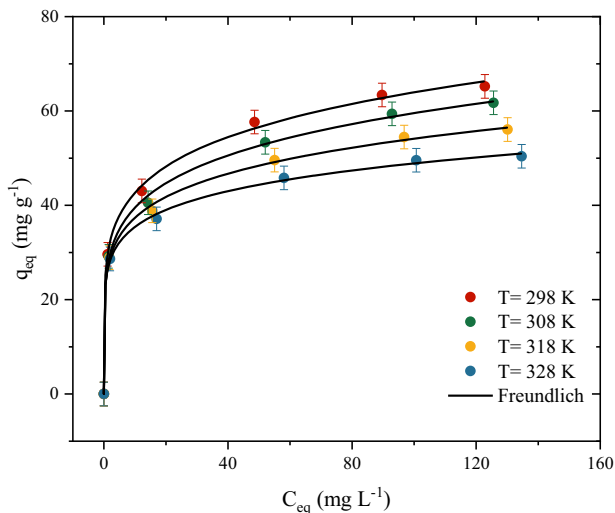


Fig. 4 Equilibrium adsorption data and Freundlich model prediction for PCM adsorption on activated carbon according to the system temperature ($T = 298, 308, 318$ and 328 K, $\text{pH } 3$, $D_{\text{ads}} = 0.8 \text{ g L}^{-1}$, $t = 180 \text{ min}$)

binding sites, which tends to increase. On the other hand, the inverse effect was found for the adsorption capacity, where the values decreased from 47.78 to 33.30 mg g^{-1} , this effect is easily explained by the inverse relation of the batch adsorption equations. The intersection point of the curve can be used as an indicator of the ideal dosage for the system. Which, in this case, it was found to be 0.8 g L^{-1} , at this point the capacity was 42.08 mg g^{-1} and removal 69.39% , respectively. Thus this dosage was selected to be further employed in the remaining adsorption experiments.

Adsorption Isotherms and Thermodynamic Parameters for the Adsorption of PCM onto the Activated Carbon

The isotherm data (Fig. 4) was constructed to obtain information regarding the effect of the temperature on the equilibrium between the PCM on the solution and the surface of the activated carbon. The first aspect to be noted is that the increase of the system temperature from 298 K to 328 K causes a decrease in the adsorption capacity, from 66.27 to 50.95 mg g^{-1} . This indicates that the nature of the adsorption is exothermic. Aiming at the development of an adsorbent to be applied in the future under real conditions, this is a positive point since its adsorption capacity is favored at room temperature (289 K). This unfavorable behavior due to the increase in system temperature is widely reported in the literature since most adsorbents developed for PCM removal perform better at temperatures close to 298 K (Kerkhoff et al. 2021; Norouzi et al. 2018; Spaltro et al. 2021). The second aspect is related to the equilibrium of the isotherm, it is possible to observe that the adsorption

capacity can still increase with the concentration. In other words, the system did not reach a plateau for the concentration range studied.

Aiming to obtain information regarding the adsorption process, the following isotherm models were fitted to the experimental data: Langmuir, Freundlich, Dubinin–Radushkevich, and Tempkin, the estimated parameters are shown in (Table 1). The most suitable model was chosen on basis of the statistical parameters. The Freundlich model was found to be a better model for representing the experimental data, achieving the highest values for correlation coefficient ($R^2 > 0.99$), adjusted coefficient of determination ($R^2_{\text{adj}} > 0.99$) and lowest values of ARE ($< 1.73\%$), and MSR ($< 12 \text{ mg g}^{-1}$). The Tempkin model also obtained good values of statistical coefficients, being the second-best fitted model. The last models were Langmuir and Dubinin–Radushkevich, showing the least satisfactory statistical indicators. Even so, the Langmuir model presented a maximum adsorption capacity close to the experimental one. From the works in the literature with drugs, it is found that several studies presented a good fit to the Freundlich isotherm, this behavior may be related to the low concentrations that are normally carried out in the studies and also the presence of a heterogeneous surface providing adsorption in multilayer (Phasuphan et al. 2019; López-Cázares et al. 2021).

The maximum experimental adsorption capacity of the adsorbent of 65 mg g^{-1} was used to compare its performance with other existing adsorbents in the literature on PCM adsorption. Analyzing Table S2, the material developed showed the sixth-best adsorption capacity ($Q_{\text{max}} = 65 \text{ mg g}^{-1}$, referring to the experimental capacity). Other adsorbents that show better performance are mainly activated carbons. Being possible to observe that the activating agent plays an important role in the maximum adsorption capacity. The highest value was found by Mashayekh-Salehi and Moussavi (Mashayekh-Salehi and Moussavi 2016), when employing NH_4Cl with activated carbon, reaching an adsorption capacity of 233 mg g^{-1} . However, the great advantage of this study is to bring a new application to the fruits of this forest species, since they generate a large volume of waste, mainly in the southern region of Brazil, where these species showed a great adaptation. Therefore, this study aims to provide the occurrence of new future work which can bring a new methodology for activated carbon preparation as well as the application in the removal of emerging pollutants.

For the determination of the thermodynamic parameters (standard Gibbs free energy change (ΔG° , kJ mol^{-1}), standard enthalpy change (ΔH° , kJ mol^{-1}), and standard entropy change (ΔS° , $\text{kJ mol}^{-1} \text{ K}^{-1}$)) - for the adsorption system, it was employed the equilibrium constant of the system, according to equations shown in the Supplementary Material.

Table 1 Equilibrium and LDF parameters of PCM adsorption on activated carbon from *Erythrina sp.* pods

Temperature (K)				
Equilibrium models	298	308	318	328
Langmuir				
q_{mL} (mg g ⁻¹)	60.83	57.18	52.42	47.72
k_L (L mg ⁻¹)	0.61	0.51	0.57	0.65
R^2	0.94	0.94	0.95	0.96
R^2_{adj}	0.91	0.91	0.92	0.94
ARE (%)	10.86	11.01	9.28	7.45
MSR (mg g ⁻¹) ²	42.65	38.67	26.29	16.16
Freundlich				
k_F ((mg g ⁻¹)(mg L ⁻¹) ^{-1/nF})	28.48	26.17	25.77	25.64
$1/n_F$ (dimensionless)	0.17	0.18	0.16	0.14
R^2	0.99	0.99	0.99	0.99
R^2_{adj}	0.99	0.99	0.99	0.99
ARE (%)	1.73	1.80	1.69	1.54
MSR (mg g ⁻¹) ²	1.20	0.93	0.73	0.54
Dubinín–Radushkevich				
q_{mDR} (mg g ⁻¹)	57.59	54.02	49.96	45.90
$\beta \times 10^7$ (kJ ² mol ⁻¹)	2.96	3.85	3.94	3.85
R^2	0.91	0.91	0.92	0.94
R^2_{adj}	0.85	0.84	0.87	0.91
ARE (%)	10.96	11.18	9.67	7.97
MSR (mg g ⁻¹) ²	71.34	63.64	42.64	25.90
Tempkin				
a (mg g ⁻¹)	313.32	339.79	408.67	511.12
b (L mg ⁻¹)	29.15	24.43	39.98	90.75
R^2	0.98	0.97	0.98	0.98
R^2_{adj}	0.77	0.77	0.81	0.86
ARE (%)	2.72	3.31	2.59	1.84
MSR (mg g ⁻¹) ²	4.00	4.79	2.86	1.47
LDF Model				
	Initial Concentration (mg L ⁻¹)			
	25	50	100	
q_{exp} (mg g ⁻¹)	29.61	45.04	55.68	
q_{pred} (mg g ⁻¹)	29.67	45.18	57.40	
C_{exp} (mg L ⁻¹)	1.30	13.96	55.44	
C_{pred} (mg L ⁻¹)	1.25	13.85	54.07	
$k_{LDF} \times 10^4$ (s ⁻¹)	5.50	5.66	8.54	
$D_S \times 10^9$ (cm ² s ⁻¹)	2.00	2.06	3.11	
R^2	0.943	0.966	0.960	
ARE (%)	8.72	7.50	8.08	
MSE (mg g ⁻¹) ²	5.74	8.01	14.68	

Table 2 Thermodynamic parameters of PCM adsorption on activated carbon from *Erythrina sp.* pods

T(K)	K_c (-)	ΔG^0 (kJ mol ⁻¹)	ΔH^0 (kJ mol ⁻¹)	ΔS^0 (kJ mol ⁻¹ K ⁻¹)
298.15	71741.61	-27.71	-39.11	-0.05
308.15	37441.40	-26.98		
318.15	26831.91	-26.97		
328.15	13122.64	-25.87		

found at 298 K. Thus indicating that the adsorption tends to be favored at low temperatures. Furthermore, the negative values of the standard Gibbs free energy change implies the adsorption is spontaneous and favorable process, not requiring the addition of any external energy. A negative value of standard enthalpy change, indicate that the adsorption process of the PCM onto the activated carbon has an exothermic nature. In addition, the magnitude of the ΔH^0 value (-39.11 kJ mol⁻¹) is consistent with a mechanism involving electrostatic interactions between the adsorbent and the adsorbate (value between 20 and 80 kJ mol⁻¹). Regarding the ΔS^0 , (-0.05 kJ mol⁻¹ K⁻¹) the negative value shows that the disturbance of the system at the solid-liquid interface decreased during adsorption (Bonilla-Petriciolet et al. 2017). Last, ΔH^0 contributed more than $\Delta S^0 T$ to the negative values of ΔG^0 , suggesting that adsorption is an enthalpy-controlled process (Crini and Badot 2008).

Kinetic Profile and LDF Model

Figure 5 shows the kinetic curves of the PCM/activated carbon system and represents the time required to achieve the equilibrium for different concentrations about the adsorption capacity (Fig. S5a) and concentration decay (Fig. 5B). The curves in adsorption capacity and concentration are equivalent to the time, where it is possible to observe that for the lower initial concentration (25 mg.L⁻¹), the equilibrium tends to be reached around 120 min, which corresponds to the equilibrium adsorption capacity of 27.64 mg g⁻¹ and a concentration equilibrium of 1.3 mg L⁻¹. For the higher concentration (50 and 100 mg L⁻¹) the equilibrium tends to reach around 80 min, reaching an adsorption capacity of 43.0 and 53.71 mg g⁻¹ and equilibrium concentration of 13.96 and 55.44 mg L⁻¹. Overall the adsorption and decay curves showed similar behavior, reaching the equilibrium after a determined time. The first minutes of the adsorption kinetics is attributed to the external mass transfer. This behavior has already been reported in other studies when also applying activated carbon derived from plant residues (Georgin et al. 2022). It is noteworthy, that the increase in the equilibrium time with the initial concentration indicates that the surface diffusion

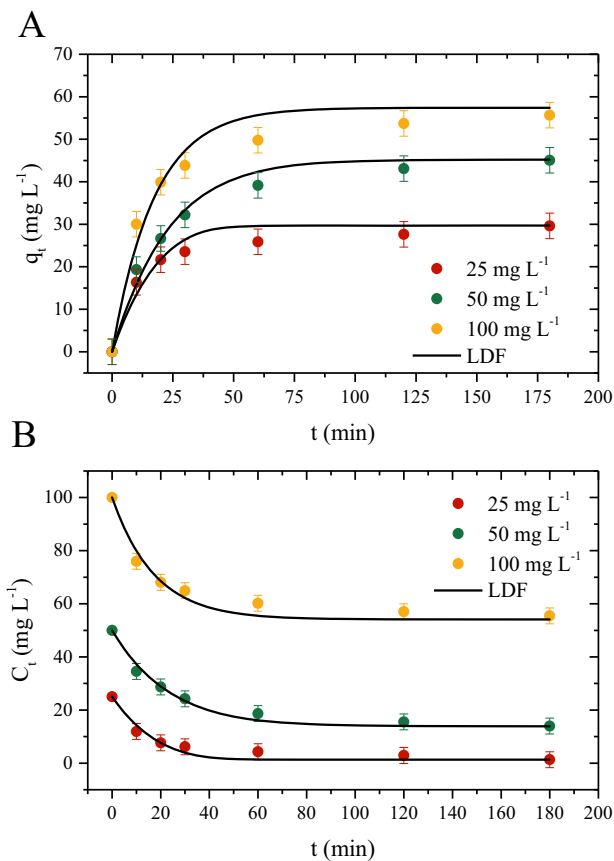


Fig. 5 PCM adsorption kinetic curves on activated carbon ($T = 298$ K, $D_{\text{ads}} = 0.8$ g L⁻¹, $\text{pH} = 3$, $V = 50$ mL). **A** q_t versus t . **B** C_t versus t

mechanism tends to increase with the initial concentration. This effect is explained by the initial concentration which causes a higher concentration gradient that leads to a higher adsorption rate at the surface of the adsorbent, thus increasing the surface diffusion, this is further corroborated by the estimated surface diffusion values (Ruthven 1984; Sudo et al. 1978).

Aiming to obtain more information regarding the adsorption mechanism, the LDF was fitted to the experimental data, the results are shown in Table 1. The model presented a good statistical fit to the experimental data with good statistical parameters, obtaining good values of $R^2 \geq 0.94$; and low values of $\text{MSE} \leq 14.68$ (mg g⁻¹)² and $\text{ARE} \leq 8.72\%$. In addition, the adsorption capacity values of the model were close to those obtained experimentally, being 57.4, 9.67, and 45.18 mg g⁻¹ as the concentration increased. The minimum concentrations obtained were 1.26, 13.85, and 54.08 mg L⁻¹ for concentrations of 25, 50, and 100 mg L⁻¹, respectively. Regarding the mass transfer coefficient (K_{LDE}) it was observed that it had a slight increase from 5.50 to 8.54 min⁻¹, showing that it was little influenced by the increase in PCM concentration. The surface diffusion also increased with increasing concentration,

ranging from 2.01 to 3.12×10^{-4} cm² s⁻¹. Both behaviors are similar to those observed by Georgin et al., (Georgin et al. 2021) when analyzing the adsorption of ketoprofen on activated carbon. As previously explained the increase of the diffusion parameter indicates that as the concentration increases the concentration gradient is higher as the adsorption rate at the surface (Worch 2012).

Propose of the Adsorption Mechanism

In this section, the adsorption mechanism is further discussed taking into account the results obtained from the characterization, pH effect, molecule aspects (speciation and dimer formation), and thermodynamic parameters it is possible to propose an adsorption mechanism. Starting with the adsorbent, in general, activated carbon is formed by C-C, C-H, C=O, and C-OH, which possibilities the hydrogen bonding, electrostatic interaction, and π - π interaction (Dougherty 2013). Furthermore, the pH_{pzc} was determined to ensure that the proposal of the adsorption mechanism is correct. As displayed in the supplementary material, it was found that the $\text{pH}_{\text{pzc}} = 6.2$, meaning that when the solution pH is below 6.2, the surface of the adsorbent will be positively charged. Second, at pH 3 the PCM is mainly found in the neutral form since the transition to ionization at pH 7. Last, the thermodynamic values indicate that the nature of the adsorption is due to the physical interactions. Overall it is expected that at acid pH most of the surface of the activated carbon has a positive charge, due to carbon protonation, and that PCM molecule in its neutral form can perfume hydrogen bonding, electrostatic interaction, and cation- π interaction, as demonstrated in Fig. 6.

Simulated Effluent Treatment

The spectrum for the solution before and after the treatment is depicted in Fig. 7. Through, the difference between the area under each curve is possible to observe that the activated carbon was able to diminish the concentration of the mixture, (from the PCM and the other compounds) achieving removal of 76.45%. It is noteworthy that, the pod is residual biomass found in large quantities in Brazil, indicating that higher quantities of the material should not be a problem for the application. Regarding the percentage of removal Georgin et al., (Georgin et al. 2021), also prepared activated charcoal with pods of the *Jacaranda mimosifolia* species and obtained the removal of 71.4% in a drug mixture containing ketoprofen and ibuprofen. Kerkhoff et al., (Kerkhoff et al. 2021), prepared activated charcoal using the endocarp of *Butia capitata* and found the removal of 84.82% in a synthetic mixture containing ketoprofen, ibuprofen, paracetamol, and naproxen.

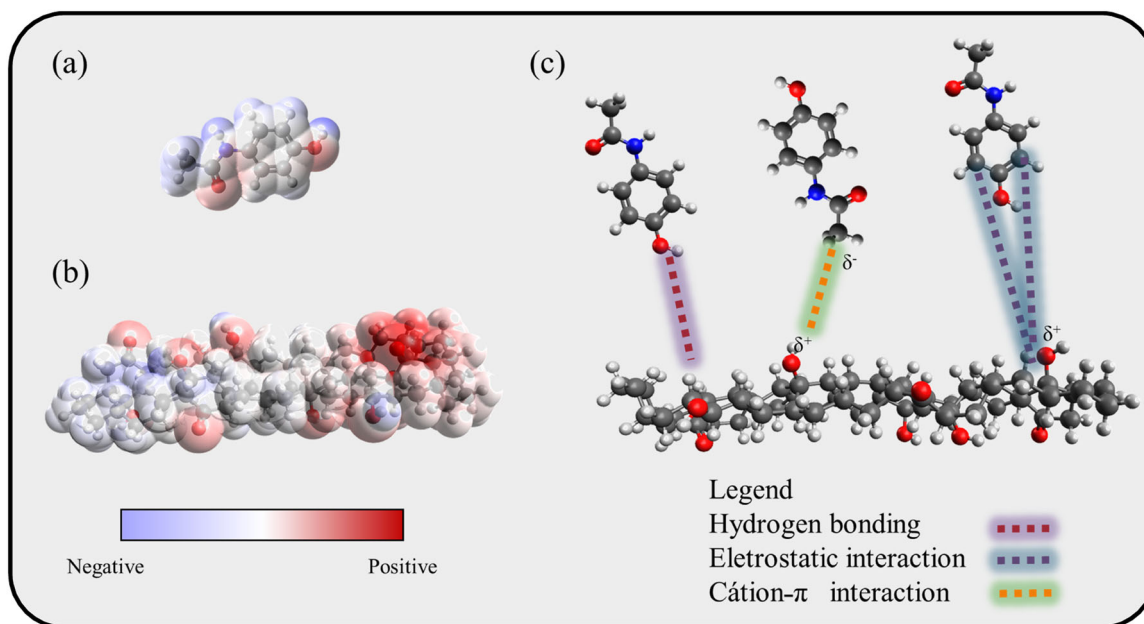


Fig. 6 **a** PCM electrostatic potential, **b** activated carbon electrostatic potential, **c** adsorption mechanism of the PCM onto the activated carbon

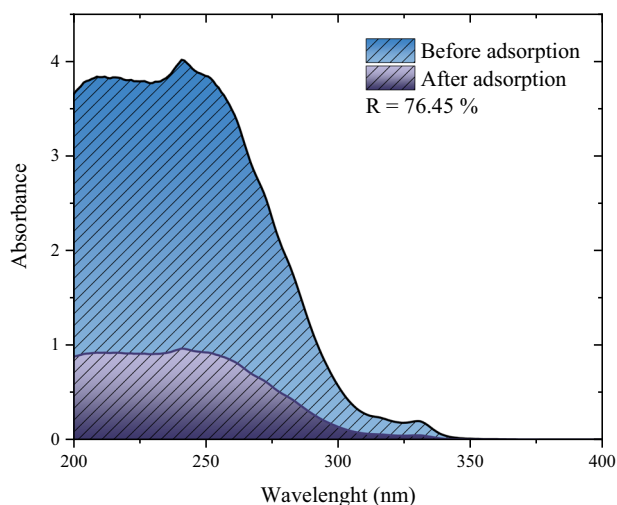


Fig. 7 Spectra for the simulated effluent before and after the adsorption treatment ($T = 298\text{ K}$, adsorbent dosage = 2 g L^{-1} , $\text{pH} = 6.5$, stirring rate = 180 rpm , $V = 100\text{ mL}$)

Conclusion

Residual pods of the forest species *Erythrina sp.* were successfully pyrolyzed with ZnCl_2 and applied to remove the drug paracetamol in an aqueous solution. The adsorption results can be associated with properties of the activated carbon such as high surface area, pores, and the surface functional groups such as C-H and C-OH. The highest adsorption capacity was found at acid pH which is justified by the speciation. The maximum adsorption capacity at equilibrium was found to be 65.0 mg g^{-1} at pH

3, 298 K . The temperature caused a diminishing effect on the adsorption capacity, with the Freundlich model being able to describe the adsorption equilibrium at all different temperatures. From the thermodynamic nature, it was found that paracetamol is spontaneously adsorbed, and presents an exothermic nature. It was found that the equilibrium time is independent of the studied concentrations, being reached after 120 min of contact, presenting an adsorption capacity high as 55.60 mg g^{-1} for the initial concentration of 100 mg L^{-1} . The linear driving force model was able to describe the adsorption and decay curves, presenting values close to the experimental one for all the studied concentrations. The characterization and thermodynamic results indicate that paracetamol tends to be adsorbed due to electrostatic interactions, hydrogen bonds, and cation- π interaction. The treatment of the simulated effluent found that the activated carbon was able to adsorb 76.45% of PCM. Overall, the activated carbon from the residual *Erythrina sp.* pods shows to be promising regarding its future applicability, since it was efficient in the adsorption of the target molecule and possible application in the treatment of mixtures.

Author Contributions JG: conceptualization, investigation, resources, writing - original draft. DSPF: conceptualization, methodology, formal analysis. MSN: conceptualization, writing - review & editing. MSM: conceptualization, writing - review & editing. MZ: conceptualization, writing - review & editing. LM: conceptualization, methodology, formal analysis, writing - original draft, visualization, writing - review & editing. DGAP: conceptualization, methodology, formal analysis, writing - original draft, visualization, writing - review & editing. LFOS: conceptualization, methodology, formal analysis, writing - original draft, visualization, writing - review & editing.

Compliance with Ethical Standards

Conflict of Interest The authors declare no competing interests.

References

- Addamo M, Augugliaro V, Di Paola A, García-López E, Loddo V, Marci G, Palmisano L (2005) Removal of drugs in aqueous systems by photoassisted degradation. *J Appl Electrochem* 35:765–774. <https://doi.org/10.1007/s10800-005-1630-y>
- Adebisi GA, Chowdhury ZZ, Alaba PA (2017) Equilibrium, kinetic, and thermodynamic studies of lead ion and zinc ion adsorption from aqueous solution onto activated carbon prepared from palm oil mill effluent. *J Clean Prod* 148:958–968. <https://doi.org/10.1016/j.jclepro.2017.02.047>
- Afolabi IC, Popoola SI, Bello OS (2020) Modeling pseudo-second-order kinetics of orange peel-paracetamol adsorption process using artificial neural network. *Chemom Intell Lab Syst* 203:104053. <https://doi.org/10.1016/j.chemolab.2020.104053>
- Alagha O, Manzar MS, Zubair M, Anil I, Mu'azu ND, Qureshi A (2020) Magnetic Mg-Fe/LDH intercalated activated carbon composites for nitrate and phosphate removal from wastewater: insight into behavior and mechanisms. *Nanomaterials* 10:1361
- Álvarez-Torrellas S, Rodríguez A, Ovejero G, García J (2016) Comparative adsorption performance of ibuprofen and tetracycline from aqueous solution by carbonaceous materials. *Chem Eng J* 283:936–947. <https://doi.org/10.1016/j.cej.2015.08.023>
- Baldoni AB, Botin AA, Tardin FD, de Barros Marques JA, de Oliveira FL, Silva AJR, da Silva ES, Awabdi CP, Filho EP, Neves LG, de Andrea Pantaleão A, Teodoro LPR, Teodoro PE (2020) Early selection strategies in schizolobium parahyba var. amazonicum (huber ex ducke) barneby. *Ind Crops Prod* 152:112538. <https://doi.org/10.1016/j.indcrop.2020.112538>
- Bello OS, Moshood MA, Ewetumo BA, Afolabi IC (2020) Ibuprofen removal using coconut husk activated Biomass. *Chem Data Collect* 29:100533. <https://doi.org/10.1016/j.cdc.2020.100533>
- Benyekkou N, Ghezzer MR, Abdelmalek F, Addou A (2020) Elimination of paracetamol from water by a spent coffee grounds biomaterial. *Environ Nanotechnol, Monit Manag* 14:100396. <https://doi.org/10.1016/j.enmm.2020.100396>
- Bernal V, Giraldo L, Moreno-Piraján JC (2021) Understanding the solid-liquid equilibria between paracetamol and activated carbon: Thermodynamic approach of the interactions adsorbent-adsorbate using equilibrium, kinetic and calorimetry data. *J Hazard Mater* 419:126432. <https://doi.org/10.1016/j.jhazmat.2021.126432>
- Bertolini A, Ferrari A, Ottani A, Guerzoni S, Tacchi R, Leone S (2006) Paracetamol: New vistas of an old drug. *CNS Drug Rev* 12:250–275. <https://doi.org/10.1111/j.1527-3458.2006.00250.x>
- Blaisi NI, Zubair M, Ihsanullah S, Ali TS, Kazeem MS, Manzar W, Al-Kutti MA, Al Harthi (2018) Date palm ash-MgAl-layered double hydroxide composite: sustainable adsorbent for effective removal of methyl orange and eriochrome black-T from aqueous phase. *Environ Sci Pollut Res* 25:34319–34331. <https://doi.org/10.1007/s11356-018-3367-2>
- Bonilla-Petriciolet A, Mendoza-Castillo DI, Reynel-Ávila HE (2017) Adsorption processes for water treatment and purification. *Adsorpt Process Water Treat Purif* 1–256. <https://doi.org/10.1007/978-3-319-58136-1>
- Chakraborty JN (2014) 30 – Differential coloured effect in dyeing, in: *Fundam. Pract. Colouration Text* 391–417. <https://doi.org/10.1016/B978-93-80308-46-3.50030-3>
- Crini G, Badot P-MM (2008) Application of chitosan, a natural aminopolysaccharide, for dye removal from aqueous solutions by adsorption processes using batch studies: A review of recent literature. *Prog Polym Sci* 33:399–447. <https://doi.org/10.1016/j.progpolymsci.2007.11.001>
- Cruz GJF, Piriñá M, Matějová L, Ainassaari K, Solis JL, Fajgar R, Šolcová O, Keiski RL (2018) Two unconventional precursors to produce ZnCl₂-Based activated carbon for water treatment applications. *Chem Eng Technol* 41:1649–1659. <https://doi.org/10.1002/ceat.201800150>
- P.D. da, C. Kemerich, W.F. de Borba, N. Schmachtenberg, C. Graepin, C.E.B. Flores, G. Barros, Chemical changes in soil occupied for cemetery horizontal in Rio Grande do Sul - North, (2014)
- Dai Y, Zhang N, Xing C, Cui Q, Sun Q (2019) The adsorption, regeneration and engineering applications of biochar for removal organic pollutants: A review. *Chemosphere* 223:12–27. <https://doi.org/10.1016/j.chemosphere.2019.01.161>
- Danish M, Ahmad T, Hashim R, Said N, Akhtar MN, Mohamad-Saleh J, Sulaiman O (2018) Comparison of surface properties of wood biomass activated carbons and their application against rhodamine B and methylene blue dye, Elsevier B.V. <https://doi.org/10.1016/j.surfin.2018.02.001>
- de H, Gomes O, de Tarso P, Freire C, do Nascimento RF, Pereira Teixeira RN (2022) Removal of contaminants from water using Moringa oleifera Lam. as biosorbent: An overview of the last decade. *J Water Process Eng* 46:102576. <https://doi.org/10.1016/j.jwpe.2022.102576>
- de P, Amaral A, Antunes AR, Barlow JW (2019) Isolation of erythrinan alkaloids from the leaves and flowers of *Erythrina speciosa*. *Rev Bras Farmacogn* 29:488–490. <https://doi.org/10.1016/j.bjp.2019.01.007>
- de YLDO, Salomón O, Georgin J, Franco DSP, Netto MS, Picilli DGA, Foletto EL, Oliveira LFS, Dotto GL (2021) High-performance removal of 2,4-dichlorophenoxyacetic acid herbicide in water using activated carbon derived from Queen palm fruit endocarp (*Syagrus romanzoffiana*). *J Environ Chem Eng* 9:104911. <https://doi.org/10.1016/j.jece.2020.104911>
- Dougherty DA (2013) The cation- π interaction. *Acc Chem Res* 46:885–893. <https://doi.org/10.1021/ar300265y>
- Dubinin MM, Astakhov VA, Bering BP, Gordeeva VA, Dubinin MM, Efimova LI, Serpinski VV (1971) Development of concepts of the volume filling of micropores in the adsorption of gases and vapors by microporous adsorbents - Communication 4. Differential heats and entropies of adsorption. *Bull Acad Sci USSR Div Chem Sci* 20:17–22. <https://doi.org/10.1007/BF00849310>
- Fahmy NM, Al-Sayed E, El-Shazly M, Singab AN (2018) Comprehensive review on flavonoids biological activities of *Erythrina* plant species. *Ind Crops Prod* 123:500–538. <https://doi.org/10.1016/j.indcrop.2018.06.028>
- Ferreira RC, de Lima HHC, Cândido AA, Junior OMC, Arroyo PA, Gauze GF, Carvalho KQ, Barros MASD(2015) Adsorption of paracetamol using activated carbon of dende and babassu coconut mesocarp *Int J Biol Biomol Agric Food Biotechnol Eng* 9:575–580. [waset.org/Publication/10001579](https://doi.org/10.1007/978-3-319-58136-1)
- Fessard V, Le Hégarat L (2010) A strategy to study genotoxicity: Application to aquatic toxins, limits and solutions. *Anal Bioanal Chem* 397:1715–1722. <https://doi.org/10.1007/s00216-010-3699-3>
- Fontana KB, Chaves ES, Sanchez JDSS, Watanabe ERLRLR, Pirotbelli JMTATA, Lenzi GG (2016) Textile dye removal from aqueous solutions by malt bagasse: Isotherm, kinetic and thermodynamic studies. *Ecotoxicol Environ Saf* 124:329–336. <https://doi.org/10.1016/j.ecoenv.2015.11.012>
- Franco DSP, Georgin J, Netto MS, Allasia D, Oliveira MLS, Foletto EL, Dotto GL (2021) Highly effective adsorption of synthetic phenol effluent by a novel activated carbon prepared from fruit wastes of the Ceiba speciosa forest species. *J Environ Chem Eng* 9:105927. <https://doi.org/10.1016/j.jece.2021.105927>
- Franco DSP, Vieillard J, Salau NPG, Dotto GL (2020) Interpretations on the mechanism of In(III) adsorption onto chitosan and chitin:

- A mass transfer model approach. *J Mol Liq* 304:112758. <https://doi.org/10.1016/j.molliq.2020.112758>
- Freundlich H (1907) Über die Adsorption in Lösungen, *Zeitschrift Für Phys. Chemie.* 57U. <https://doi.org/10.1515/zpch-1907-5723>
- Georgin J, Boit Martinello Kda, Franco DSP, Netto MS, Piccilli DGA, Yilmaz M, Silva LFO, Dotto GL (2022) Residual peel of pitaya fruit (*Hylocereus undatus*) as a precursor to obtaining an efficient carbon-based adsorbent for the removal of metanil yellow dye from water. *J Environ Chem Eng* 10. <https://doi.org/10.1016/j.jece.2021.107006>
- Georgin J, de YL, Salomón O, Franco DSP, Netto MS, Piccilli DGA, Perondi D, Silva LFO, Foletto EL, Dotto GL (2021) Development of highly porous activated carbon from *Jacaranda mimosifolia* seed pods for remarkable removal of aqueous-phase ketoprofen. *J Environ Chem Eng* 9:105676. <https://doi.org/10.1016/j.jece.2021.105676>
- Georgin J, Dotto GL, Mazutti MA, Foletto EL (2016) Preparation of activated carbon from peanut shell by conventional pyrolysis and microwave irradiation-pyrolysis to remove organic dyes from aqueous solutions. *J Environ Chem Eng* 4:266–275. <https://doi.org/10.1016/j.jece.2015.11.018>
- Glueckauf E (1955) Theory of chromatography. Part 10.—Formule for diffusion into spheres and their application to chromatography. *Trans Faraday Soc* 51:1540–1551. <https://doi.org/10.1039/TF9555101540>
- Goscianska J, Olejnik A, Ejsmont A, Galarza A, Wuttke S (2021) Overcoming the paracetamol dose challenge with wrinkled mesoporous carbon spheres. *J Colloid Interface Sci* 586:673–682. <https://doi.org/10.1016/j.jcis.2020.10.137>
- Guo W, Fu Y, Jia R, Guo Z, Su C, Li J, Zhao X, Jin Y, Li P, Fan J, Zhang C, Qu P, Cui H, Gao S, Cheng H, Li J, Li X, Lu B, Xu X, Wang Z (2022) Visualization of the infection risk assessment of SARS-CoV-2 through aerosol and surface transmission in a negative-pressure ward. *Environ Int* 162:107153. <https://doi.org/10.1016/j.envint.2022.107153>
- Han Q, Wang J, Goodman BA, Xie J, Liu Z (2020) High adsorption of methylene blue by activated carbon prepared from phosphoric acid treated eucalyptus residue. *Powder Technol* 366:239–248. <https://doi.org/10.1016/j.powtec.2020.02.013>
- Hollender J, Singer H, McArdell CS (2008) Polar Organic Micropollutants. In: Hlavinek P, Bonacci O, Marsalek J, Mahrikova I (Eds.) *The Water Cycle BT - Dangerous Pollutants (Xenobiotics) in Urban Water Cycle*. Springer, Netherlands, Dordrecht, p 103–116. in:
- Husin NA, Muhamad M, Yahaya N, Miskam M, Syazni Nik Mohamed Kamal NN, Asman S, Raov M, Mohamad Zain NN (2021) Application of a new choline-imidazole based deep eutectic solvents in hybrid magnetic molecularly imprinted polymer for efficient and selective removal of naproxen from aqueous samples. *Mater Chem Phys* 261:124228. <https://doi.org/10.1016/j.matchemphys.2021.124228>
- Jari Y, Roche N, Necibi MC, El Hajjaji S, Dhiba D, Chehbouni A (2022) Emerging pollutants in moroccan wastewater: occurrence, impact, and removal technologies. *J Chem* 2022:9727857. <https://doi.org/10.1155/2022/9727857>
- Katibi KK, Yunus KF, Che Man H, Aris AZ, bin Mohd Nor MZ, binti Azis RS (2021) Recent advances in the rejection of endocrine-disrupting compounds from water using membrane and membrane bioreactor technologies: a review. *Polymers (Basel)* 13. <https://doi.org/10.3390/polym13030392>
- Kerkhoff CM, da Boit Martinello K, Franco DSP, Netto MS, Georgin J, Foletto EL, Piccilli DGA, Silva LFO, Dotto GL (2021) Adsorption of ketoprofen and paracetamol and treatment of a synthetic mixture by novel porous carbon derived from *Butia capitata* endocarp. *J Mol Liq* 339:117184. <https://doi.org/10.1016/j.molliq.2021.117184>
- Khan AH, Khan NA, Zubair M, Azfar Shaida M, Manzar MS, Abutaleb A, Naushad M, Iqbal J (2022) Sustainable green nano-adsorbents for remediation of pharmaceuticals from water and wastewater: A critical review. *Environ Res* 204:112243. <https://doi.org/10.1016/j.envres.2021.112243>
- Khetan SK, Collins TJ (2007) Human pharmaceuticals in the aquatic environment: A challenge to green chemistry. *Chem Rev* 107:2319–2364. <https://doi.org/10.1021/cr020441w>
- Klavarioti M, Mantzavinos D, Kassinos D (2009) Removal of residual pharmaceuticals from aqueous systems by advanced oxidation processes. *Environ Int* 35:402–417. <https://doi.org/10.1016/j.envint.2008.07.009>
- Kong X, Gao H, Song X, Deng Y, Zhang Y (2020) Adsorption of phenol on porous carbon from *Toona sinensis* leaves and its mechanism. *Chem Phys Lett* 739:137046. <https://doi.org/10.1016/j.cplett.2019.137046>
- Konozy EHE, Bernardes ES, Rosa C, Faca V, Greene LJ, Ward RJ (2003) Isolation, purification, and physicochemical characterization of a D-galactose-binding lectin from seeds of *Erythrina speciosa*. *Arch Biochem Biophys* 410:222–229. [https://doi.org/10.1016/S0003-9861\(02\)00695-1](https://doi.org/10.1016/S0003-9861(02)00695-1)
- Langmuir I (1918) The adsorption of gases on plane surfaces of glass, mica and platinum. *J Am Chem Soc* 40:1361–1403. <https://doi.org/10.1021/ja02242a004>
- Lazarotto JS, Boit Martinello Kda, Georgin J, Franco DSP, Netto MS, Piccilli DGA, Silva LFO, Lima EC, Dotto GL (2021) Preparation of activated carbon from the residues of the mushroom (*Agaricus bisporus*) production chain for the adsorption of the 2,4-dichlorophenoxyacetic herbicide. *J Environ Chem Eng* 9. <https://doi.org/10.1016/j.jece.2021.106843>
- Li Y, Wang Y, He L, Meng L, Lu H, Li X (2020) Preparation of poly(4-vinylpyridine)-functionalized magnetic Al-MOF for the removal of naproxen from aqueous solution. *J Hazard Mater* 383:121144. <https://doi.org/10.1016/j.jhazmat.2019.121144>
- Liakos EV, Rekos K, Giannakoudakis DA, Mitropoulos AC, Fu J, Kyzas GZ (2021) Activated porous carbon derived from tea and plane tree leaves biomass for the removal of pharmaceutical compounds from wastewaters. *Antibiotics* 10. <https://doi.org/10.3390/antibiotics10010065>
- Lima DR, Hosseini-Bandegharaei A, Thue PS, Lima EC, de Albuquerque YRT, dos Reis GS, Umpierrez CS, Dias SLP, Tran HN (2019) Efficient acetaminophen removal from water and hospital effluents treatment by activated carbons derived from Brazil nutshells. *Colloids Surf A Physicochem Eng Asp* 583:123966. <https://doi.org/10.1016/j.colsurfa.2019.123966>
- López-Cázares MI, Isaacs-Páez ED, Ascacio-Valdés J, Aguilar-González CN, Rangel-Mendez JR, Chazaro-Ruiz LF (2021) Electro-assisted naproxen adsorption followed by its electrodegradation and simultaneous electroreactivation of the activated carbon electrode. *Sep Purif Technol* 258. <https://doi.org/10.1016/j.seppur.2020.118030>
- Madden JC, Enoch SJ, Hewitt M, Cronin MTD (2009) Pharmaceuticals in the environment: Good practice in predicting acute ecotoxicological effects. *Toxicol Lett* 185:85–101. <https://doi.org/10.1016/j.toxlet.2008.12.005>
- Manzar MS, Zubair M, Khan NA, Husain Khan A, Baig U, Aziz MA, Blaisi NI, Abdel-Magid HIM (2020) Adsorption behaviour of green coffee residues for decolorization of hazardous congo red and eriochrome black T dyes from aqueous solutions. *Int J Environ Anal Chem.* <https://doi.org/10.1080/03067319.2020.1811260>
- Martín J, Buchberger W, Santos JL, Alonso E, Aparicio I (2012) High-performance liquid chromatography quadrupole time-of-flight mass spectrometry method for the analysis of antidiabetic drugs in aqueous environmental samples. *J Chromatogr B Anal Technol Biomed Life Sci* 895–896:94–101. <https://doi.org/10.1016/j.jchromb.2012.03.023>

- Mashayekh-Salehi A, Moussavi G (2016) Removal of acetaminophen from the contaminated water using adsorption onto carbon activated with NH₄Cl. *Desalin Water Treat* 57:12861–12873. <https://doi.org/10.1080/19443994.2015.1051588>
- Medina CL, Sanches MC, Tucci MLS, Sousa CAF, Cuzzuol GRF, Joly CA (2009) *Erythrina speciosa* (Leguminosae-Papilionoideae) under soil water saturation: Morphophysiological and growth responses. *Ann Bot* 104:671–680. <https://doi.org/10.1093/aob/mcp159>
- Mestre AS, Tyszko E, Andrade MA, Galhetas M, Freire C, Carvalho AP (2015) Sustainable activated carbons prepared from a sucrose-derived hydrochar: remarkable adsorbents for pharmaceutical compounds. *RSC Adv* 5:19696–19707. <https://doi.org/10.1039/C4RA14495C>
- Nandan A, Siddiqui NA, Singh C, Aeri A, Gwenzi W, Ighalo JO, de Carvalho Nagliate P, Meili L, Singh P, Chaukura N, Rangabhashiyam S (2021) COVID-19 pandemic in Uttarakhand, India: Environmental recovery or degradation. *J Environ Chem Eng* 9:106595. <https://doi.org/10.1016/J.JECE.2021.106595>
- Neuwoehner J, Escher BI (2011) The pH-dependent toxicity of basic pharmaceuticals in the green algae *Scenedesmus vacuolatus* can be explained with a toxicokinetic ion-trapping model. *Aquat Toxicol* 101:266–275. <https://doi.org/10.1016/j.aquatox.2010.10.008>
- Norouzi S, Heidari M, Alipour V, Rahmanian O, Fazlzadeh M, Mohammadi-moghadam F, Nourmoradi H, Goudarzi B, Dindarlo K (2018) Preparation, characterization and Cr(VI) adsorption evaluation of NaOH-activated carbon produced from Date Press Cake; an agro-industrial waste. *Bioresour Technol* 258:48–56. <https://doi.org/10.1016/j.biortech.2018.02.106>
- Ocampo-Perez R, Padilla-Ortega E, Medellín-Castillo NA, Coronado-Oyarvide P, Aguilar-Madera CG, Segovia-Sandoval SJ, Flores-Ramírez R, Parra-Marfil A (2019) Synthesis of biochar from chili seeds and its application to remove ibuprofen from water. Equilibrium and 3D modeling. *Sci Total Environ* 655:1397–1408. <https://doi.org/10.1016/j.scitotenv.2018.11.283>
- Ogunmodede J, Akanji SB, Bello OS (2021) Moringa oleifera seed pod-based adsorbent for the removal of paracetamol from aqueous solution: A novel approach toward diversification. *Environ Prog/Sustain Energy* 40:e13615. <https://doi.org/10.1002/ep.13615>
- Oksman K, Mathew AP, Bondeson D, Kvien I (2006) Manufacturing process of cellulose whiskers/poly(lactic acid) nanocomposites. *Compos Sci Technol* 66:2776–2784. <https://doi.org/10.1016/j.compscitech.2006.03.002>
- Pereira MFR, Soares SF, Órfão JJM, Figueiredo JL (2003) Adsorption of dyes on activated carbons: Influence of surface chemical groups. *Carbon N. Y* 41:811–821. [https://doi.org/10.1016/S0008-6223\(02\)00406-2](https://doi.org/10.1016/S0008-6223(02)00406-2)
- Phasuphan W, Praphairaksit N, Imyim A (2019) Removal of ibuprofen, diclofenac, and naproxen from water using chitosan-modified waste tire crumb rubber. *J Mol Liq* 294:111554. <https://doi.org/10.1016/j.molliq.2019.111554>
- Pi N, Ng JZ, Kelly BC (2017) Bioaccumulation of pharmaceutically active compounds and endocrine disrupting chemicals in aquatic macrophytes: Results of hydroponic experiments with *Echinodorus horemanii* and *Eichhornia crassipes*. *Sci Total Environ* 601–602:812–820. <https://doi.org/10.1016/j.scitotenv.2017.05.137>
- Puchana-Rosero MJ, Adebayo MA, Lima EC, Machado FM, Thue PS, Vaghetti JCP, Umpierrez CS, Gutierrez M (2016) Microwave-assisted activated carbon obtained from the sludge of tannery-treatment effluent plant for removal of leather dyes. *Colloids Surf A Physicochem Eng Asp* 504:105–115. <https://doi.org/10.1016/j.colsurfa.2016.05.059>
- D.U. Quintela, D.C. Henrique, P.V. dos, S. Lins, A.H. Ide, A. Erto, J.L. da S. Duarte, L. Meili, Waste of *Mytella Falcata* shells for removal of a triarylmethane biocide from water: Kinetic, equilibrium, regeneration and thermodynamic studies, *Colloids Surfaces B Biointerfaces*. 195 (2020). <https://doi.org/10.1016/j.colsurfb.2020.111230>
- Rahman A, Hango HJ, Daniel LS, Uahengo V, Jaime SJ, Bhaskaruni SVHS, Jonnalagadda SB (2019) Chemical preparation of activated carbon from *Acacia erioloba* seed pods using H₂SO₄ as impregnating agent for water treatment: An environmentally benevolent approach. *J Clean Prod* 237:117689. <https://doi.org/10.1016/j.jclepro.2019.117689>
- Rakić V, Rac V, Krmar M, Otman O, Auroux A (2015) The adsorption of pharmaceutically active compounds from aqueous solutions onto activated carbons. *J Hazard Mater* 282:141–149. <https://doi.org/10.1016/j.jhazmat.2014.04.062>
- Ruthven DM (1984) Principles of adsorption and adsorption processes, 7th ed. John Wiley & Sons, Berlin. [https://doi.org/10.1016/0167-6989\(85\)90037-6](https://doi.org/10.1016/0167-6989(85)90037-6)
- Salomón YL, Georgin J, Franco DSP, Netto MS, Picilli DGA, Foletto EL, Pinto D, Oliveira MLS, Dotto GL (2022) Adsorption of atrazine herbicide from water by diospyros kaki fruit waste activated carbon. *J Mol Liq* 347:117990. <https://doi.org/10.1016/j.molliq.2021.117990>
- Saood Manzar M, Ahmad T, Ullah N, Velayudhaperumal Chellam P, John J, Zubair M, Brandão RJ, Meili L, Alagha O, Çevik E (2022) Comparative adsorption of Eriochrome Black T and Tetracycline by NaOH-modified steel dust: Kinetic and process modeling. *Sep Purif Technol* 287:120559. <https://doi.org/10.1016/j.seppur.2022.120559>
- Siedlecka EM, Ofiarska A, Borzyszkowska AF, Białk-Bielińska A, Stepnowski P, Pieczyńska A (2018) Cytostatic drug removal using electrochemical oxidation with BDD electrode: Degradation pathway and toxicity. *Water Res* 144:235–245. <https://doi.org/10.1016/j.watres.2018.07.035>
- Sivarajasekar N, Mohanraj N, Sivamani S, Prakash Maran J, Ganesh Moorthy I, Balasubramani K (2018) Statistical optimization studies on adsorption of ibuprofen onto Albizialebeck seed pods activated carbon prepared using microwave irradiation. *Mater Today Proc* 5:7264–7274. <https://doi.org/10.1016/j.matpr.2017.11.394>
- Sohrabi C, Alsafi Z, O'Neill N, Khan M, Kerwan A, Al-Jabir A, Iosifidis C, Agha R (2020) World Health Organization declares global emergency: A review of the 2019 novel coronavirus (COVID-19). *Int J Surg* 76:71–76. <https://doi.org/10.1016/j.ijsu.2020.02.034>
- Soto-Hernandez M, Jackson AH (1994) *Erythrina* alkaloids: Isolation and characterisation of alkaloids from seven *Erythrina* species. *Planta Med* 60:175–177. <https://doi.org/10.1055/s-2006-959445>
- Spaltro A, Pila MN, Colasurdo DD, Noseda Grau E, Román G, Simonetti S, Ruiz DL (2021) Removal of paracetamol from aqueous solution by activated carbon and silica. Experimental and computational study. *J Contam Hydrol* 236:103739. <https://doi.org/10.1016/j.jconhyd.2020.103739>
- Spessato L, Bedin KC, Cazetta AL, Souza IPAF, Duarte VA, Crespo LHS, Silva MC, Pontes RM, Almeida VC (2019) KOH-super activated carbon from biomass waste: Insights into the paracetamol adsorption mechanism and thermal regeneration cycles. *J Hazard Mater* 371:499–505. <https://doi.org/10.1016/j.jhazmat.2019.02.102>
- Streit AFMM, Collazzo GC, Druzian SP, Verdi RS, Foletto EL, Oliveira LFSS, Dotto GL (2021) Adsorption of ibuprofen, ketoprofen, and paracetamol onto activated carbon prepared from effluent treatment plant sludge of the beverage industry. *Chemosphere* 262:128322. <https://doi.org/10.1016/j.chemosphere.2020.128322>
- Sudo Y, Mistic DM, Suzuki M (1978) Concentration dependence of effective surface diffusion coefficient in aqueous phase

- adsorption on activated carbon. *Chem Eng Sci* 33:1287–1290. [https://doi.org/10.1016/0009-2509\(78\)85097-0](https://doi.org/10.1016/0009-2509(78)85097-0)
- Sundaraman S, Aravind Kumar J, Deivasigamani P, Devarajan Y (2022) Emerging pharma residue contaminants: Occurrence, monitoring, risk and fate assessment – A challenge to water resource management. *Sci Total Environ* 825:153897. <https://doi.org/10.1016/j.scitotenv.2022.153897>
- Temkin M, Pyzhev V (1939) Kinetics of the synthesis of ammonia on promoted iron catalysts. *Jour Phys Chem (U S S R)* 13:851–867
- Tran HN, Wang YF, You SJ, Chao HP (2017) Insights into the mechanism of cationic dye adsorption on activated charcoal: The importance of π - π interactions. *Process Saf Environ Prot* 107:168–180. <https://doi.org/10.1016/j.psep.2017.02.010>
- Tunç MS, Yıldız B, Taşar Ş (2021) Removal of paracetamol from aqueous solution by wood sawdust-derived activated carbon: Process optimization using response surface methodology. *Chem Eng Commun* 0:1–21. <https://doi.org/10.1080/00986445.2021.1978075>
- Wang Z, Li Y, Hu M, Lei T, Tian Z, Yang W, Yang Z, Graham NJD (2022) Influence of DOM characteristics on the flocculation removal of trace pharmaceuticals in surface water by the successive dosing of alum and moderately hydrophobic chitosan. *Water Res* 213:118163. <https://doi.org/10.1016/j.watres.2022.118163>
- Wong S, Lim Y, Ngadi N, Mat R, Hassan O, Inuwa IM, Mohamed NB, Low JH (2018) Removal of acetaminophen by activated carbon synthesized from spent tea leaves: equilibrium, kinetics and thermodynamics studies. *Powder Technol* 338:878–886. <https://doi.org/10.1016/j.powtec.2018.07.075>
- Worch E (2012), Adsorption technology in water treatment: Fundamentals, processes, and modeling. <https://doi.org/10.1515/9783110240238>
- Xu J, Chen W, Wu L, Chang AC (2009) Adsorption and Degradation of Ketoprofen in Soils. *J Environ Qual* 38:1177–1182. <https://doi.org/10.2134/jeq2008.0347>
- Zhang Y, Shao D, Yan J, Jia X, Li Y, Yu P, Zhang T (2016) The pore size distribution and its relationship with shale gas capacity in organic-rich mudstone of Wufeng-Longmaxi Formations, Sichuan Basin, China. *J Nat Gas Geosci* 1:213–220. <https://doi.org/10.1016/j.jnggs.2016.08.002>
- Zubair M, Manzar MS, Mu'azu ND, Anil I, Blaisi NI, Al-Harhi MA (2020) Functionalized MgAl-layered hydroxide intercalated date-palm biochar for Enhanced Uptake of Cationic dye: Kinetics, isotherm and thermodynamic studies. *Appl Clay Sci* 190:105587. <https://doi.org/10.1016/j.clay.2020.105587>
- Zubair M, Manzar MS, Suleiman MA, Fernandes DP, Meili L, Bin Essa WA, Al-Adam H, AlGhamdi JM, Mu'azu ND, Haladu SA, Khan G (2022) Production of magnetic biochar-steel dust composites for enhanced phosphate adsorption. *J Water Process Eng* 47:102793. <https://doi.org/10.1016/j.jwpe.2022.102793>
- Žur J, Wojcieszynska D, Hupert-Kocurek K, Marchlewicz A, Guzik U (2018) Paracetamol – toxicity and microbial utilization. *Pseudomonas moorei* KB4 as a case study for exploring degradation pathway. *Chemosphere* 206:192–202. <https://doi.org/10.1016/j.chemosphere.2018.04.179>

Publisher's note Springer Nature remains neutral with regard to jurisdictional claims in published maps and institutional affiliations.

Springer Nature or its licensor holds exclusive rights to this article under a publishing agreement with the author(s) or other rightsholder(s); author self-archiving of the accepted manuscript version of this article is solely governed by the terms of such publishing agreement and applicable law.